IBRACON Structures and Materials Journal
Revista IBRACON de Estruturas e Materiais
ISSN 1983-4195 ismj.org

ORIGINAL ARTICLE

M-N interaction curves for rectangular concrete-filled steel tube columns subjected to uniaxial bending moments

Curvas de interação M-N para pilares mistos preenchidos de seção retangular sujeitos a flexão composta reta

Matheus Fernandes[a]
Silvana De Nardin[a]
Fernando Menezes de Almeida Filho[a]

[a]Universidade Federal de São Carlos – UFSCar, Programa de Pós-graduação em Engenharia Civil, São Carlos, SP, Brasil

Received 11 March 2021
Accepted 26 May 2021

Abstract: In this paper, a computational code was developed to obtain M-N interaction curves for rectangular concrete-filled steel tube columns considering the strain compatibility in the cross-section. Considering the composite section subjected to uniaxial bending moments, expressions were developed to determine normal force, moment resistance, neutral axis depth and components resistance of cross-section. Such expressions were implemented in a computational tool developed to the authors and that allows to obtain the M-N pairs of strength. The steel and concrete ultimate strains were defined with the aid of the Brazilian standard for reinforced concrete structures ABNT NBR 6118. The obtained results were compared to simplified curves defined according to the theoretical models of ABNT NBR 8800, ABNT NBR 16239, EN 1994-1-1 and literature data. The proposed model showed good agreement with literature results and had good precision to estimate the ultimate moment values. To further understand the resistance of composite columns under uniaxial bending moments, parametric study was performed to evaluate the influence of the compressive strength of concrete, yielding strength of steel and steel area ratio on M-N interaction curves. The results indicate that the yielding strength of steel and the steel area ratio were the variables that most influenced the values of composite columns resistance (normal force and bending moment).

Keywords: concrete-filled steel tube column, uniaxial bending moment, M-N interaction curve.

Resumo: Neste trabalho é proposto um processo computacional para obtenção de curvas de interação M-N para pilares mistos preenchidos de seção retangular, por meio da compatibilidade de deformações na seção transversal. Considerando flexão composta reta, foram desenvolvidas expressões que relacionam esforço normal, momento resistente, profundidade da linha neutra e resistência dos componentes da seção transversal. Tais expressões foram implementadas em uma ferramenta computacional que possibilita a definição dos pares resistentes M-N. As deformações específicas últimas de compressão do concreto e de tração no aço foram definidas com auxílio da norma brasileira para estruturas de concreto armado ABNT NBR 6118. Para verificação do processo elaborado, os resultados obtidos foram confrontados com curvas simplificadas traçadas de acordo com os modelos da ABNT NBR 8800, ABNT NBR 16239 e EN 1994-1-1 e com resultados da literatura. O modelo proposto apresentou boa concordância com resultados da literatura e estimou, com boa precisão, os momentos resistentes últimos. Por meio de um estudo paramétrico foi avaliada a influência da resistência à compressão do concreto, resistência ao escoamento do aço e taxa de aço nas curvas de interação M-N. Os resultados mostraram que a resistência ao escoamento do aço e a taxa de aço foram as variáveis que mais influenciaram nos valores resistentes (força normal e momento fletor).

Palavras-chave: pilar misto preenchido, flexão composta reta, curva de interação M-N.

How to cite: M. Fernandes, S. De Nardin, and F. M. Almeida Filho, "M-N interaction curves for rectangular concrete-filled steel tube columns subjected to uniaxial bending moments," *Rev. IBRACON Estrut. Mater.*, vol. 15, no. 1, e15108, 2022, https://doi.org/10.1590/S1983-41952022000100008

Corresponding author: Matheus Fernandes. E-mail: matheustkful@gmail.com
Financial support: None.
Conflict of interest: Nothing to declare.

1 INTRODUCTION

The concrete-filled steel tube columns have been widely used for construction in several countries due to their high resistant capacity, unnecessary of formwork and reinforcing bars and simplified construction process, resulting in saving and high execution speed. Such characteristics highlight this type of column in relation to both the steel and reinforced concrete columns. In this type of column, the steel tube is filled by concrete, assuming two main shapes: rectangular and circular. Both in the rectangular and circular sections there are great constructive advantages, reducing expenses related to the concreting process. From a structural point of view, the concrete-filled steel tube columns allow a better use of the concrete, due to the confinement effect provided by the steel profile. Such an effect is more significant in the circular concrete-filled steel tube columns [1].

Several numerical and experimental studies have evaluated the influence of parameters on the capacity of concrete-filled steel tube columns. Therefore, it is important to understand the structural behavior of such an element under a specific request, which allows a better use of the element. Uniaxial bending moment in concrete-filled steel tube columns has been extensively evaluated, several parameters such as the compressive strength of concrete, yielding strength of steel and eccentricities of axial force are widely evaluated in many studies. The first studies on rectangular concrete-filled steel tube columns subject to eccentric compression date from the 1960s [2], 1970s [3] e 1980s [4], [5]. Since then, many studies have investigated the influence of parameters such as eccentricity, slenderness, yielding strength of steel and compressive strength of concrete on the eccentric compression strength of the concrete-filled steel tube columns. About the eccentricities of normal force, a significant reduction in the ultimate force was observed with the increase in the eccentricity [6]–[9]. Experimental results showed that the reduction in ultimate force occurs due to the increase in flexural buckling [4], [10]; the effects of flexural buckling are even more significant when the element is subjected to uniaxial bending moment about the minor axis [4]. The increase in the compressive strength of concrete also has a direct influence on the eccentric compression strength; the greater the compressive strength of concrete the greater the resistant capacity of the column [11]–[14]. However, the use of high-strength concretes significantly reduces the ductility of the column [11], [14], while the use of concretes of strength below 50 MPa favors the ductility [15]. Like the effect caused by the variation in the compressive strength of concrete, the increase in the yielding strength of steel also increases the eccentric compression strength of the column [16]–[19]. For certain eccentricity values, regardless of the shape of the filled section, a small increase was observed in the eccentric compression strength [16]. For example, by varying the yield strength of steel from 488 to 690 MPa, increases of 27% and 30% were observed for ultimate values of force and moment, respectively [18]. The results showed that the increase in the eccentric compression strength of the rectangular concrete-filled steel tube column is more significant as there is a successive increase in the yielding strength of steel [17].

Standard codes as ABNT NBR 8800 [20], ABNT NBR 16239 [21] and EN 1994-1-1 [22] present simplified procedures for the design of composite columns under eccentric loads. Such simplifications may not accurately represent the properties of the components of composite section [23], but the use of that is very simple and practice [24]. The main simplification adopted is the linearization of the diagrams using straight lines. Although this is a procedure that greatly simplifies the design/verification process, it can be quite a distance from the real response. Studies based on experimental analyzes show that technical standards, in general, conservatively estimate the eccentric compression strength [25]–[27]. When comparing such simplified diagrams that consider a plastic stress distribution with results obtained by strain compatibility, the simplified results were shown to be non-conservative and with considerable error for rectangular concrete-filled steel tube columns with the use of high-strength steel [28]. Another important aspect is the Brazilian standard code [20] limits the compressive strength of concrete to 50 MPa. On the other hand, the Brazilian code for reinforced concrete elements [29] allows the use of concrete up to 90 MPa. Thus, in the present study, a software was developed to predict the M-N interaction curve of rectangular concrete-filled section considering the strain compatibility and concrete strength between 20 and 90 MPa. Moreover, the influence of compressive strength of concrete (f_c), yielding strength of steel tube (f_y) and steel ratio was investigated in this study. The influence of these parameters on the interaction curve shape and resistance of concrete-filled steel tube column under eccentric load were evaluated in the present study. In addition, the parabolic interaction diagrams were compared to design interaction diagrams of the Brazilian [20], [21] and European [22] standard codes and with literature responses [17], [18].

2 SIMPLIFIED M-N INTERACTION STRENGTH

The Brazilian standard code for steel and composite structures [20] presents two simplified models for verify the composite columns subjected to eccentric compression; both assume the plastic stress distribution. The Model I is based on the American standard code for steel structures [30] while the Model II is based on the European standard for

composite structures [22]. The verification of M-N interaction strength using Model I is done using a simplified curve (Figure 1a) composed of two parts: line passing through points A and B; another passing through points B and C. Such a model provides for a 10% reduction in the design value of plastic resistance moment ($M_{pl,\,Rd}$) to obtain the design value of resistance moment (M_{Rd}). The M-N interaction model presented in the Brazilian standard code for steel and composite structures with use of tubular profiles [21] is like Model I [20]. However, points A and B of the M-N interaction diagram have the same value of resistance moment (Figure 1b).

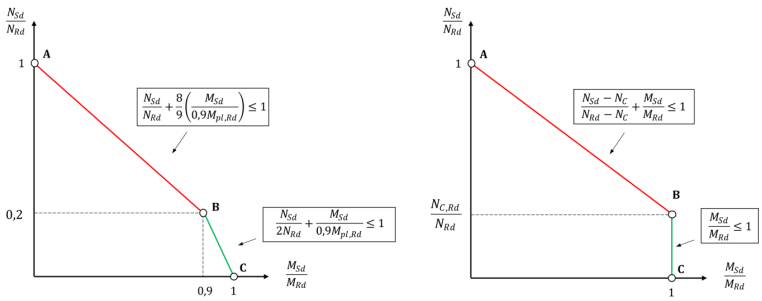

a) Model I for M-N interaction. Adapted from ABNT NBR 8800 [20].

b) Model for M-N interaction. Adapted from ABNT NBR 16239 [21].

Figure 1. Models for M-N interaction: ABNT NBR 8800 [20] and ABNT NBR 16239 [21].

In addition, the Model I and takes into account the effects of flexural buckling using the parameter χ (Equation 1 and Equation 2) for resistance of composite column under compressive normal force (N_{Rd}). The M-N interaction model presented by ABNT NBR 16239 [21] also considers the effects of flexural buckling, but in a less conservative way (Parameter χ, Figure 1b).

$$\chi = 0,658^{\lambda_o{}^2},\ for\ \lambda_o \leq 1,5 \tag{1}$$

$$\chi = \frac{0,877}{\lambda_o^2},\ for\ \lambda_o > 1,5 \tag{2}$$

where λ_o = relative slenderness of composite column.

The Model II is similar to EN 1994-1-1 [22] model and the M-N interaction curve is represented by three parts (Figure 2).

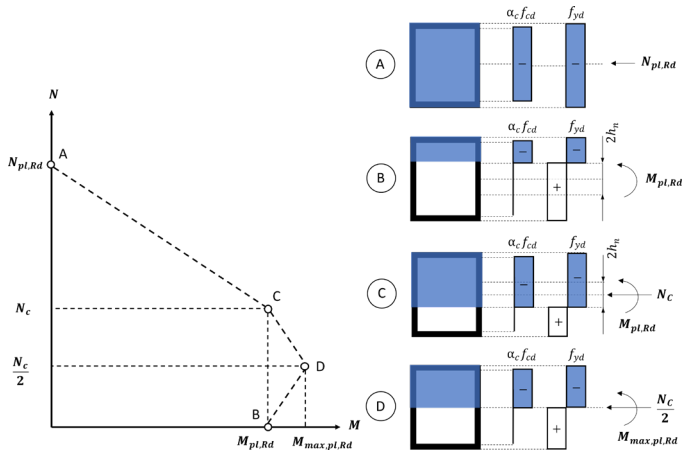

Figure 2. Model II for M-N interaction. Adapted from EN 1994-1-1 [22].

The α_c coefficient is considered equal to 0,85 by ABNT NBR 8800 [20]. The Brazilian standard [20] does not consider the effects of concrete confinement for filled rectangular sections; in the proposed model α_c coefficient is defined with the aid of Equation 6. The European standard [22] considers a specific formulation for filled circular sections, for better consideration of the concrete confinement effect. On the other hand, in filled rectangular sections, EN 1994-1-1 [22] considers α_c equal to 1. In the present study, the simplified curves of strength considering the two models (I and II) presented by Brazilian Standard code [20] and the curves of strength presented by ABNT NBR 16239 [21], are compared to parabolic curves obtained from the strain compatibility for rectangular concrete-filled steel tube column.

3 CONSTRUCTION OF AXIAL FORCE-MOMENT INTERACTION CURVES

Strain compatibility method assumes two main hypotheses: 1) plane sections remain plane; 2) steel-concrete full-composite action. Following the assumption of strain compatibility and linear strain distribution over the entire cross-section, the M-N pair of strength is defined from the variation of the neutral axis depth: a depth of neutral axis is arbitrated, and the M-N pair of strength is obtained for that, considering the composite section subjected to uniaxial bending moment. The process is analogous to the commonly used in reinforced concrete sections and it follows the steps: description of cross-section equilibrium using equilibrium equations, calculation of components strains in function of the neutral axis depth, considering the flexural buckling parameter. By shifting the neutral axis position consecutively, numerous combinations of axial force N and bending moment M can be generated and the full range of interaction diagrams from pure compression to pure bending can be traced by the software developed by the authors. The main steps are detailed in the next items.

3.1 Equilibrium equations of cross-section

The resulting forces in the composite section, regarding to the steel profile and concrete, are shown in Figure 3. Equation 3 and Equation 4 define the M-N pair of strength (Table 1), where x is the neutral axis depth.

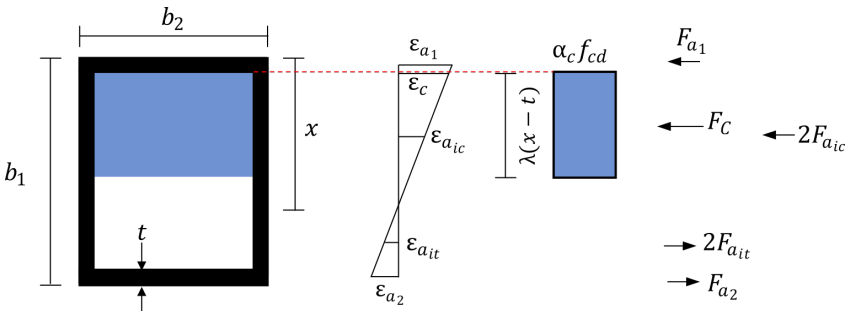

Figure 3. Resulting forces on components of rectangular composite cross-section.

Table 1. M-N pair of cross-section strength.

Plastic resistance to compression, $N_{pl,Rd}$	
$$N_{pl,Rd} = \lambda(x-t)(b_2-2t)(-\alpha_c f_{cd}) - \sigma_{a_1} A_{a_1} + \sigma_{a_2} A_{a_2} - \sum_{i=1}^{n} 2\sigma_{a_{ic}} A_{a_{ic}} + \sum_{i=1}^{n} 2\sigma_{a_{it}} A_{a_{it}}$$	(3)
Resistance moment, M_{Rd}	
$$M_{Rd} = \lambda(x-t)(b_2-2t)\left(\frac{b_1}{2} - \frac{\lambda(x-t)}{2} - t\right)(-\alpha_c f_{cd}) - \sigma_{a_1} A_{a_1} y_{a1} + \sigma_{a_2} A_{a_2} y_{a_2} - \sum_{i=1}^{n} 2\sigma_{a_{ic}} A_{a_{ic}} y_{aic} + \sum_{i=1}^{n} 2\sigma_{a_{it}} A_{a_{it}} y_{ait}$$	(4)

where σ_a = stress on portion of steel section (kN/cm^2); y_a = distance between the gravity center of a portion of steel and the gravity center of the cross-section (cm); A_a , A_{ai} = portion area of flanges of the steel profile and infinitesimal area of steel tube, respectively (cm^2); and f_{cd} = design value of compressive strength of concrete (kN/cm^2).

The coefficients λ and α_c are defined according to ABNT NBR 6118 [29] and shown in Equation 5 and Equation 6.

$$\lambda = 0,8 - \frac{f_c - 50}{400} \leq 0,8 \quad (5)$$

$$\alpha_c = 0,85\left[1 - \frac{f_c - 50}{200}\right] \leq 0,85 \quad (6)$$

where f_c = compressive strength of concrete (MPa).

If the normal force is not prevalent in the cross-section, as in concrete, plastic behavior was adopted, the proposed model may not adequately represent the real situation. Despite this, the simplified models of ABNT NBR 8800 [20] and EN 1994-1-1 [22] also consider plastic behavior of concrete. Such simplification is coherent, as in columns the axial force is generally high.

3.2 Strains in composite cross-section

Stresses acting on steel components (σ_i, Equation 7 and Equation 8) are defined from the strains. The linear elastic behavior and validity of Hooke's Law are considered for strains less than or equal to ε_{ydi} (Equation 7). For strains higher than ε_{ydi}, the stresses in the steel components are limited by the yielding strength of steel (f_{ydi}), as shown in Equation 8. The strains in cross-section (ε_i) are calculated according to the strain region: Region I, II and III (Figure 4), according to coefficient β_x (Equation 9).

$$\sigma_i = \varepsilon_i E_i, \ for\ \varepsilon_i \leq \varepsilon_{y_{di}} \quad (7)$$

$$\sigma_i = f_{yd_i}, \ for\ \varepsilon_i > \varepsilon_{y_{di}} \quad (8)$$

$$\beta_x = \frac{x}{d_s} \quad (9)$$

where E_i = modulus of elasticity of steel component i (kN/cm^2); d_s = effective depth of the cross-section (cm); and $\varepsilon_{y_{di}}$ = steel design yield strain of steel component i (dimensionless).

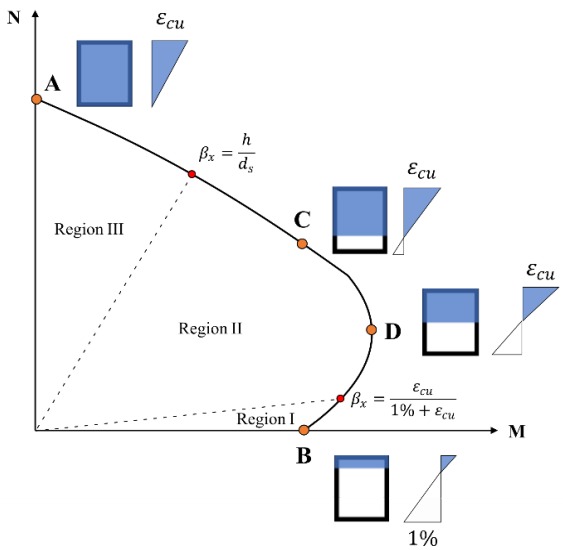

Figure 4. Strain limits for strain regions of composite cross-section.

The ultimate value of concrete compressive strain ε_{cu} (Table 2) is defined according to the recommendations of ABNT NBR 6118 [29] and depends on the compressive strength of concrete.

Table 2. Ultimate values-concrete compressive strains. Adapted from ABNT NBR 6118 [29].

Concrete strength classes	Concrete strain
C20-C50	$\varepsilon_{cu} = -0,35\%$; $\varepsilon_{c2} = -0,2\ \%$
C55-C90	$\varepsilon_{cu} = -\left(0,26\% + 3,5\% \left[\frac{90 - f_c}{100} \right]^4 \right)$
	$\varepsilon_{c2} = -\left(0,2\% + 0,0085\% \left(f_c - 50 \right)^{0,53} \right)$

The ultimate strain in steel (ε_{su}) was adopted equal to 0,01 for the most external tensile steel component [29]; this defines the effective depth (d_s). The strains in the composite section depend on each strain region type (Figure 4) and are calculated with the aid of Table 3. Strains are obtained considering a horizontal layer in the cross-section (layer i).

Table 3. Strains in cross-section according to strain region.

	Cross-section	Strain in the layer i
Region I	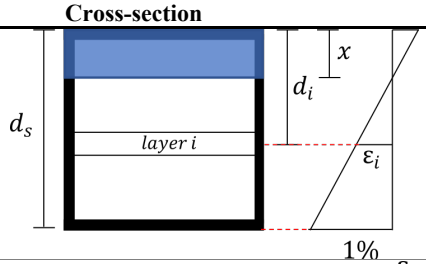	$\varepsilon_i = \frac{1\%\left(d_i - x\right)}{d_s - x}$
Region II	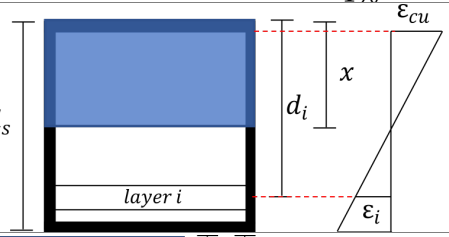	$\varepsilon_i = \frac{-\varepsilon_{cu}\left(d_i - x\right)}{x - t}$
Region III	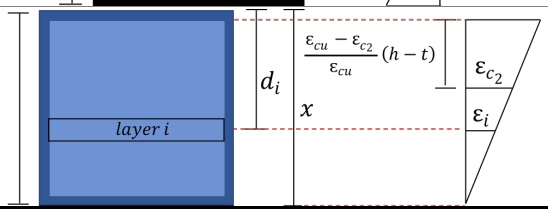	$\varepsilon_i = \frac{-\varepsilon_{c2}\left(x - d_i\right)}{x - t - \frac{\varepsilon_{cu} - \varepsilon_{c2}}{\varepsilon_{cu}}\left(h - t\right)}$

3.3 Factor reduction for buckling curve (χ)

The relevant buckling mode, considered by using the parameter χ, reduces the axial load capacity of the composite column. This can be observed in the curve that starts from point A2 (Figure 5). The reduction factor χ is depending on relative slenderness (λ_o). The M-N interaction curve of composite column and cross-section are parallel however the contour diagram of the first is smaller than the other. In present study, the flexural buckling was included on the axial load capacity using the parameter χ (Figure 5) and this same procedure was also proposed by Perea et al. [31].

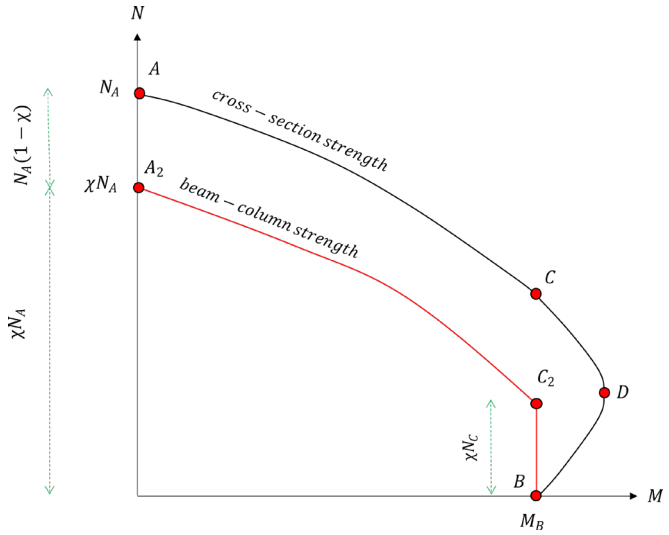

Figure 5. Reduction of plastic resistance to axial force due to flexural buckling.

Some authors present the possibility of reducing axial compressive resistance between points A and C [31], [32], and exclude the point D replacing of CDB portion by a straight-line connecting points C and B [31]. The point D on the interaction curve corresponds to the maximum moment resistance that can be achieved by the section. This is greater than M_B (uniaxial bending resistance) because the compressive axial force inhibits tensile cracking of the concrete, thus enhancing its flexural resistance. This simplification is also adopted by design curve of the Model I presented by Brazilian Standard Code [20]. Ziemian [33] proposes the reduction of the plastic resistance moment (M_B) by a coefficient equal to 0,9, like adopted by ANSI/AISC 360 [30].

In the proposed model, the reduction on plastic resistance to compression N_A was made considering the relevant buckling mode (parameter χ, Equation 1 and Equation 2) and the point D was maintained in the interaction curves. Although the consideration of point D can lead to unsafe results [34], such point was maintained so that the generated M-N interaction curve preserved its original contour resulting from the application of strain compatibility. Therefore, from these considerations, the resistance to axial force (N_{Rd}) of the rectangular concrete-filled steel tube columns, including the buckling effects in given by Equation 10, Table 4. The coefficient μ, which reduces the moment resistance, was adopted equal to 0,9 [33].

Table 4. M-N pair of strength including the reduction effects due to buckling mode.

Resistance to axial force, N_{Rd}	
$N_{Rd} = \left[\lambda(x-t)(b_2-2t)(-\alpha_c f_{cd}) - \sigma_{a_1} A_{a_1} + \sigma_{a_2} A_{a_2} - \sum_{i=1}^{n} 2\sigma_{a_{ic}} A_{a_{ic}} + \sum_{i=1}^{n} 2\sigma_{a_{it}} A_{a_{it}} \right] \chi$	(10)
Resistance moment, M_{Rd}	
$M_{Rd} = \left[\lambda(x-t)(b_2-2t)\left(\frac{b_1}{2} - \frac{\lambda(x-t)}{2} - t\right)(-\alpha_c f_{cd}) - \sigma_{a_1} A_{a_1} y_{a1} + \sigma_{a_2} A_{a_2} y_{a_2} - \sum_{i=1}^{n} 2\sigma_{a_{ic}} A_{a_{ic}} y_{aic} + \sum_{i=1}^{n} 2\sigma_{a_{it}} A_{a_{it}} y_{ait} \right] \mu$	(11)

3.4 Iterative process

Following the assumption of strain compatibility and linear strain distribution over the entire cross-section, the M-N pair of strength for each arbitrated depth can be obtained. A computational code was then developed in Visual Basic language that allow to obtain the M-N pairs of strength following the steps shown in Figure 6.

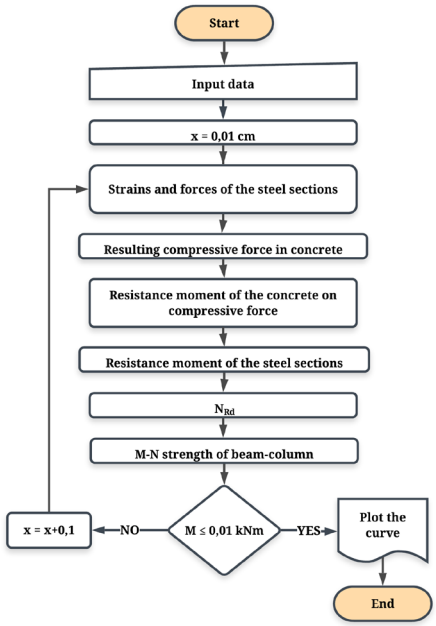

Figure 6. Iterative process of computational code.

In the verification of convergence, the computational code evaluates how close the moment resistance obtained by the equilibrium of bending moments is to point A of the interaction diagram M-N (pure compression). Is verified if the moment resistance, is less than 0,01 kN.m. If this is true, the interaction curve is plotted, because the M-N pair of strength obtained is close to Point A. Otherwise, the neutral axis is increased to by 0,1 cm and the process returns to third step (Figure 6).

The computational code was employed in a parametric study. Before that, a first analysis was done to evaluate the correlation of the results in comparison to those available in the literature. The influence of some parameters on the shape of M-N interaction diagrams was evaluates in the parametric study considering the parameters as: compressive strength of concrete, yielding strength of steel tube and the steel ratio (ratio between the area of steel tube and the concrete area in the composite section). In this study only rectangular concrete-filled steel tube columns without reinforcing bars were evaluated using the computational code. The second order effects were not taking account in the present analysis.

4 RESULTS AND DISCUSSIONS

This section presents the M-N interaction curves obtained for several rectangular concrete-filled steel tube columns. The results of M-N interaction curves were compared with simplified curves of standard codes [20]–[22] and with literature results [17], [18].

4.1 Comparison with literature responses

In this phase, the results of computational code were compared to literature results [17], [18]. In the comparative analysis with literature results, the coefficients of strength materials were adopted equal to 1,0. The simplified interaction diagrams correspond to the Brazilian Standard Codes [20], [21] and EN 1994-1-1 [22]. The simplified M- N interaction strength of the beam-column using recommendations of Brazilian Standard code [20] (Model I) interaction curve was called “Model I [20]”. These results include the consideration of reduction factor χ for the relevant buckling mode given in terms of the slenderness column.

Model II [20] and Eurocode [22] correspond to the Brazilian code [20] and EN 1994-1-1 [22], respectively. The slenderness effect of the column (Figure 5) on the M-N interaction curves is not consider by these simplified curves that consider the cross-section strength [20], [22]. In this paper, the authors included the parameter χ to taking in account the slenderness effect of columns and modified the Model II [20] and Eurocode [22] curves. The new curves were called as “Modified Model II [20]” and “Modified EN 1994-1-1 [22]” respectively (Figure 7).

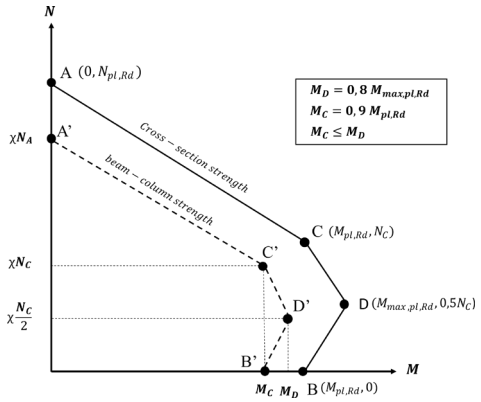

Figure 7. Modified interaction curves for Model II [20] and Eurocode [22].

The compressive resistance of the point A (Figure 7) was decreased by the slenderness reduction factor (χ) and moment values in the points B and D were also decreased considering the reductions of 0,9 or 0,8 (Figure 7). Although the Model II [20] and the Eurocode [22] are very similar, there are some differences in the partial safety factors. To the design compressive strength of concrete, the reductions are 85% and 100%, respectively from [20] and [22]. The partial safety factors for compressive strength of concrete are equal to 1,4 and 1,5, respectively for Brazilian code [20] and Eurocode [22]. The details of specimens are in Table 5.

Table 5. Validation of computational code: specimens' details of refs [17], [18].

Author	Specimen	H × B × t (mm)	f_y (MPa)	f_c (MPa)	L_e (mm)	λ_o	e (mm)	N_{exp} (kN)	M_{exp} (kNcm)
Du et al. [18]	D1	150×150×8,28	488,4	55,3	1180	0,33	0	2947	0
	D2						45	1672,5	8770
	D3						150	807,1	12970
	D4						1200	108,5	13220
Melo [17]	M1	150×150×3	250	40	1240	0,29	20	966	2445,9
	M2						30	858,3	3116,8
	M3						40	765,8	3716,0
Le: effective length									

The results of Du et al. [18] were compared to M-N curves of beam-column obtained by both proposed model and simplified interaction diagrams (Figure 8).

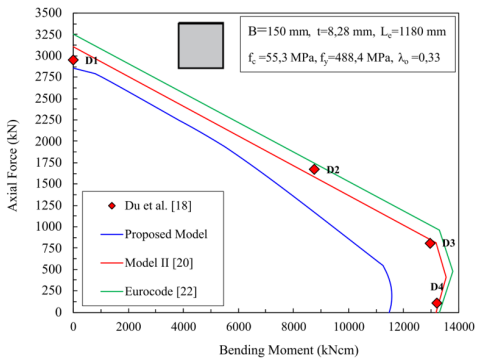

a) Proposed model *vs*. simplified M-N interaction curves (cross-section strength) *vs*. Du *et al.* [18]

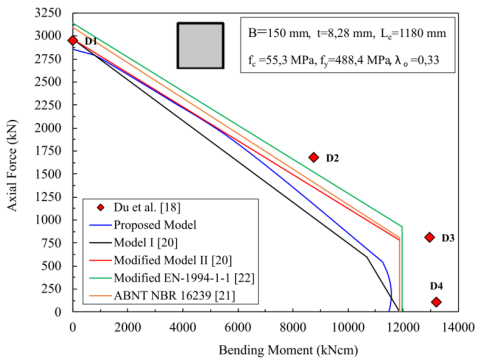

b) Proposed model *vs*. simplified M-N interaction curves (beam-column strength) *vs*. Du *et al.* [18]

Figure 8. Comparison of parabolic and simplified M-N interaction curves with results of Du et al. [18].

The estimated values of eccentric compression strength, according to model, for results of Du et al. [18] are shown in Table 6.

Table 6. Estimated values of M-N pairs of strength vs. results of Du et al. [18].

Model	D1		D2		D3		D4	
	N (kN)	M (kNm)	N (kN)	M (kNm)	N (kN)	M (kNm)	N (kN)	M (kNm)
Du et al. [18]	2947	0	1672,5	87,7	807,1	129,7	108,5	132,2
Proposed model	2855,41 (- 3,1%)	0	1451,03 (- 13,2%)	76,05 (- 13,3%)	671,17 (- 16,8%)	107,61 (- 17%)	93,15 (- 14,1%)	115,48 (- 12,6%)
Model II [20]	3107,24 (+5,4%)	0	1628,8 (- 2,6%)	85,1 (-3%)	819,18 (+1,5%)	131,71 (+1,5%)	107,67 (- 0,8%)	132,82 (+0,5%)
Eurocode [22]	3251,03 (+10,3%)	0	1711,07 (+2,3%)	89,39 (+1,9%)	834,62 (+3,4%)	134,2 (+3,5%)	108,75 (+0,2%)	134,19 (+1,5%)
Model I [20]	2969,18 (+0,8%)	0	1365,34 (- 18,4%)	71,98 (- 17,9%)	645,05 (- 20,1%)	104,55 (- 19,4%)	91,9 (- 15,3%)	116,93 (- 11,6%)
Modified Model II [20]	2969,18 (+0,8%)	0	1505,33 (- 10%)	79,35 (- 9,5%)	733,11 (- 9,2%)	118,85 (- 8,4%)	93,36 (- 14%)	118,85 (- 10,1%)
Modified EN-1994-1-1 [22]	3136 (+6,4%)	0	1588,31 (- 5%)	83,73 (- 4,5%)	739,68 (- 8,4%)	119,93 (- 7,5%)	94,02 (- 13,3%)	119,93 (- 9,3%)
ABNT NBR 16239 [21]	3098,30 (+5,1%)	0	1539,70 (- 7,9%)	80,70 (- 7,9%)	733,11 (- 9,2%)	118,85 (- 8,4%)	93,36 (- 14%)	118,85 (- 10,1%)

The results of proposed model were conservative (blue curve, Figure 8a and Table 6) and the results of simplified M-N interaction curves were unsafe when considering the cross-section strength (Figure 8a and Table 6). The simplified M-N interaction curves overestimated the value of beam-column strength to compressive normal force (N_{Rd}) in relation to the proposed model (Figure 8b); this is due the simplified models [20]–[22] take in account the plastic stress distribution. The M-N interaction curve proposed by ABNT NBR 16239 [21], presented less conservative results in relation to the interaction models of ABNT NBR 8800 [20] (Model I and Modified Model II).

The accuracy of results of proposed model in relation to compressive normal force (N_{Rd}) considering recommendations of ABNT NBR 8800 [20] (Model I and Modified Model II) was not verified for results of literature (Figure 8). In the proposed model the plastic resistance of the steel components was not reached, and this occurred because in the strain compatibility method the stress acting on steel components were obtained considering linear elastic behavior. The strains in the steel components of Du et al. [18] were lower than the strains that limit the elastic region; therefore, the yielding strength of steel was not reached for proposed model.

The results of Melo [17] are compared (Figure 9) to the proposed model and simplified diagrams of ABNT NBR 8800 [20], ABNT NBR 16239 [21] and EN 1994-1-1 [22].

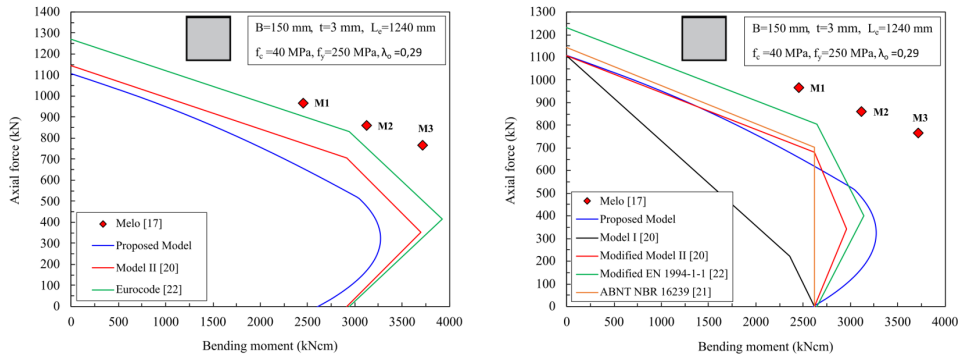

a) Proposed model *vs*. simplified M-N interaction curves (cross-section strength) *vs*. Melo [17]

b) Proposed model *vs*. simplified M-N interaction curves (beam-column strength) *vs*. Melo [17]

Figure 9. Comparison of parabolic and simplified M-N interaction curves with results of Melo [17].

The estimated values of M-N pairs of strength for results of Melo [17] are shown in Table 7.

Table 7. Estimated values of M-N pairs of strength vs. results of Melo [17].

Model	M1		M2		M3	
	N (kN)	M (kNm)	N (kN)	M (kNm)	N (kN)	M (kNm)
Melo [17]	966	24,46	858,3	31,17	765,8	37,16
Proposed model	763,56 (-21%)	19,45 (-20,5%)	663,48 (-22,7%)	24,05 (-22,8%)	575,56 (-24,8%)	27,91 (-24,9%)
Model II [20]	824,52 (-14,6%)	20,98 (-14,2%)	737,48 (-14,1%)	26,74 (-14,2%)	632,35 (-17,4%)	30,71 (-17,4%)
Eurocode [22]	917,43 (-5%)	23,29 (-4,8%)	815,33 (-5%)	29,63 (-4,9%)	677,68 (-11,5%)	32,91 (-11,4%)
Model I [20]	564,95 (-41,5%)	14,32 (-41,5%)	466,03 (-45,7%)	16,97 (-45,6%)	389,93 (-49,1%)	18,98 (-48,9%)
Modified Model II [20]	780,82 (-19,2%)	19,83 (-18,9%)	692,34 (-19,3%)	25,20 (-19,2%)	560,31 (-26,8%)	27,34 (-26,4%)
Modified EN-1994- 1- 1 [22]	868,98 (-10%)	22,11 (-9,6%)	745,36 (-13,2%)	27,17 (-12,8%)	594,73 (-22,3%)	29,02 (-21,9%)
ABNT NBR 16239 [21]	801,57 (-17,0%)	20,46 (-16,3%)	708,64 (-17,4%)	25,97 (-16,7%)	539,73 (-29,5%)	26,37 (-29,0%)

As plotted in Figure 9, a good agreement is achieved for pure bending between proposed model and the simplified M-N interaction curves when considering the beam-column strength. The results of the proposed model underestimated the resistance of all specimens [17] (Figure 9, Table 7). For beam-column strength (Figure 9b), the values of pure compressive normal force (N_{Rd}) were very close between the proposed model and the simplified curves of ABNT NBR 8800 [20]. On other hand, the value of modified EN 1994-1-1 [22] was higher than the other results (Table 7), since the European standard [22] considers 100% of the design value of compressive strength of concrete for rectangular concrete-filled steel tube columns. Additionally, the M-N interaction model proposed by ABNT NBR 16239 [21] proved to be less conservative in relation to ABNT NBR 8800 [20] (Model I and Modified Model II) for all responses in the literature [17], [18]. This is because ABNT NBR 16239 [21] considers the effects of flexural buckling in a less conservative way.

In this phase, the comparative analysis allows to observe the follow points:

- In some analyzes, the simplified models of standard codes [20], [22] allows to prevent only the cross-section strength not considering the stability reduction factor χ. This fact occurs mainly in EN 1994-1-1 [22].
- The proposed model allows to predict the M-N par of strength however the obtained values underestimated the literature responses [17], [18];
- The values of compressive normal force (N_{Rd}) obtained from proposed model were lower than that of simplified model proposed by EN 1994-1-1 [22];
- There is a strong correlation between the values of ultimate moment (M_{Rd}) resulted of proposed model and simplified models [20]–[22] when the stability factor χ (beam-column strength) was included in the interaction curves.
- The comparison between M-N pairs of strength obtained from several models including simplified models of standard codes and results of literature clearly shows the complexity of this type of analysis.

3.2 Parametric study

The parametric analysis comprised a total of three parameters: compressive strength of concrete, yielding strength of steel tube and steel ratio. Square cross-section having width of 150 mm and effective length (L_e) of 2000 mm were evaluated in this phase. When the influence of concrete strength was investigated the thickness of steel tube and the yielding strength were kept constant and equal to 3mm and 250 MPa, respectively. In this first analysis, the compressive strength of concrete varied from 20 MPa to 90 MPa in increments of 10 MPa. The yielding strength of steel was investigated considering the compressive strength of concrete equal to 20 MPa. The yielding strength of steel tube was varied from 250 MPa to 450 MPa, with increments of 50 MPa. The steel ratio was evaluated considering the thickness of steel tube equal to 4 mm, 5 mm, and 6 mm; resulting in steel ratios of 0,116, 0,178 and 0,181, respectively. Parabolic curves as well as dimensionless curves for several values of compressive strength of concrete are shown in Figure 10.

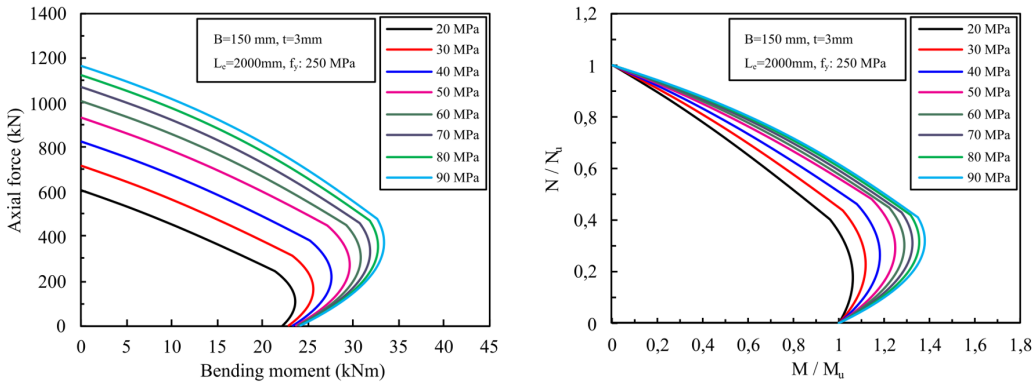

a) M-N interaction curves b) Dimensionless curves

Figure 10. Effects of concrete strength on M-N interaction curves.

The shape of the M-N diagram is highly influenced by the compressive strength of concrete. Parabolic curves are parallel to each other for all values of compressive strength of concrete. However, the offset distance between parabolic curves is higher for concretes of usual strength (20-50 MPa, Figure 10a) and becomes significantly lower when the strength of concrete is higher than 50 MPa. The increase in the compressive strength of concrete results in a significant increase of compressive normal force (N_{Rd}). On the other hand, the values of ultimate moment (horizontal axis, Figure 10a) are less sensitive to this variation. Furthermore, the increases in the M-N pairs of strength are more expressive for concretes with strengths up to 50 MPa. This fact is due to the coefficients λ and α_c are function of concrete compressive strength and the use of high-strength concretes reduces the design strength (Equation 5 and Equation 6) increasing the relative slenderness value (Equation 1 and Equation 2). The coefficient α_c (Equation 6) applied to the design value of compressive strength of concrete in accordance to Brazilian standards [20], [29] assumes a maximum value of 0,85; in contrast, the European standard [22] adopts $\alpha_c = 1$ for rectangular concrete-filled sections. This difference in the coefficient that affects the compressive strength of concrete explains the divergences of results.

The values of moment resistance at the most external point of the dimensionless interaction curves (Figure 10) were 24,9% and 37,9% higher than the ultimate moment (Point B) for values of compressive strength of 90 MPa and 50 MPa, respectively. An increase of 8,4% was observed in moment resistance at the most external point of the curve when the concrete strength varied from 20 MPa to 30 MPa, both concrete from C20-C50 class. Among the high-strength concretes, the most significant increase was 3,4% and occurred when the compressive strength varied from 60 MPa to 70 MPa. Comparing the lower and the higher values of compressive strength of concrete (C20 to C90) were observed increases of 262,9% and 41,5% in values of axial load capacity and bending moment capacity, respectively, at the most external point of the curve.

The values of the M-N pairs of strength are shown in Table 8. Comparing results of the lower and the higher values of compressive strength of concrete the axial load capacity at Point A was 92,1% higher while the bending moment capacity had an increase of only 8,9% (Point B). Therefore, an increase of compressive strength of concrete are more efficient to increase the axial load capacity and a less significant effect is observed on the values of bending moment capacity.

Table 8. Influence of concrete strength on M-N pair of strength.

Concrete (MPa)	Point A	Point B	Point D	
	N (kN)	M (kNm)	N (kN)	M (kNm)
C20	606,47	22,25	105,67	23,62
C30 (+50%)	716,69 (+18,2%)	22,91 (+2,9%)	163,7 (+54,9%)	25,62 (+8,4%)
C40 (+100%)	825,34 (+36,1%)	23,38 (+5,1%)	217,39 (+105,5%)	27,62 (+16,9%)
C50 (+150%)	932,64 (+53,8%)	23,72 (+6,6%)	272,19 (+157,6%)	29,63 (+25,4%)
C60 (+200%)	1006,68 (+66%)	23,93 (+7,5%)	304,6 (+188,2%)	30,85 (+30,6%)
C70 (+250%)	1070,19 (+76,4%)	24,07 (+8,2%)	330,86 (+213,1%)	31,89 (+35%)
C80 (+300%)	1123,42 (+85,2%)	24,18 (+8,6%)	356,98 (+237,8%)	32,75 (+38,6%)
C90 (+350%)	1165,05 (+92,1%)	24,23 (+8,9%)	383,56 (+262,9%)	33,42 (+41,5%)

In contrast to the observed for the variation of concrete strength, the interaction curves remain parallel for all values evaluated of yielding strength of steel (Figure 11a). For higher values of yielding strength, the moment resistance at Point D was closer to the ultimate moment. For the lowest value of yielding strength of steel (250 MPa) the value of moment resistance at point D was 6,2% higher than the value of ultimate moment (Figure 11b).

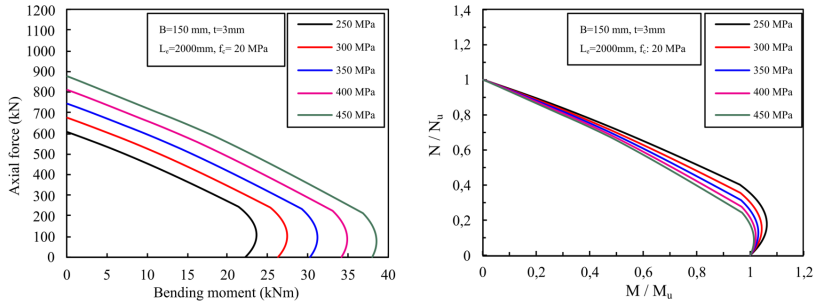

a) M-N interaction curves b) Dimensionless curves

Figure 11. Effect of yielding strength of steel on M-N interaction curves.

From the M-N pairs in the Table 9, an increase of 80% in the yielding strength results in increases of 44,6% and 71% in the axial load capacity (Point A) and pure bending moment (point B) respectively. In beam-column case (point D), it was observed an increase of 63,1% in the value of resistance moment and a reduction of 26,7% in the value of the resistance to compressive normal force when the yielding strength was increased to 450 MPa.

Table 9. Influence of yielding strength of steel on M-N pair of strength.

Yielding strength of steel (MPa)	Point A	Point B	Point D	
	N (kN)	M (kNm)	N (kN)	M (kNm)
250	606,46	22,24	106,82	23,63
300 (+20%)	675,71 (+11,4%)	26,31 (+18,3%)	102,08 (-4,4%)	27,44 (+16,1%)
350 (+40%)	743,83 (22,6%)	30,29 (+36,2%)	96,11 (-10%)	31,21 (+32,1%)
400 (+60%)	810,83 (+33,7%)	34,20 (53,8%)	85,26 (-20,2%)	34,91 (+47,7%)
450 (+80%)	876,73 (+44,6%)	38,03 (+71%)	78,32 (-26,7%)	38,55 (+63,1%)

The variation in the steel ratio significantly increased the M-N pairs of strength (Figure 12a). The increase in the steel ratio resulted in a similar effect of the yielding strength of steel: parallel curves and lower values of steel ratio resulted in more significant difference between the values of moment resistance (M_B) and ultimate moment (M_D, Figure 12b).

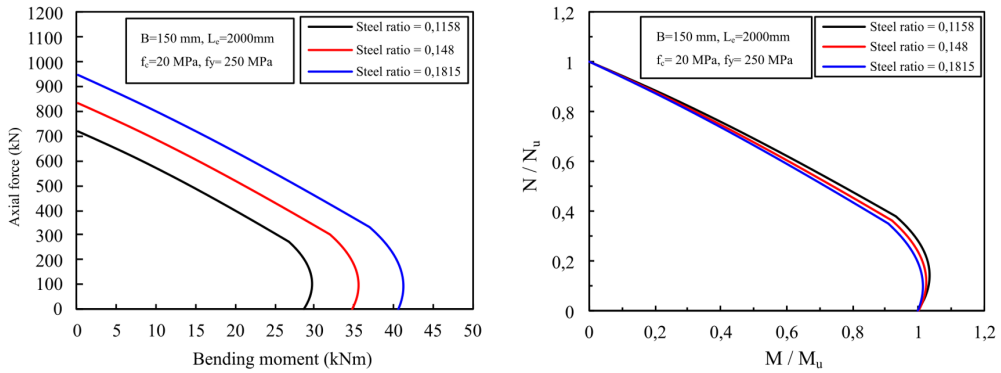

a) M-N interaction curves b) Dimensionless curves

Figure 12. Effect of steel ratio on M-N interaction curves.

When de steel ratio was increased in 50% (0,12 to 0,18, Table 10) occurred increase of 39,1% and decrease of 8,1% in the M-N pair of strength at Point D. Also, this increase in the steel ratio resulted in increase of 31,3% in axial load capacity to concentric compression (Point A, Table 10).

Table 10. Influence of steel ratio on M-N pair of strength.

Steel ratio	Point A	Point B	Point D	
	N (kN)	M (kNm)	N (kN)	M (kNm)
0,12	722,46	28,62	101,65	29,67
0,15 (+25%)	836,63 (+15,8%)	34,74 (+21,4%)	99,40 (-2,2%)	35,55 (+19,8%)
0,18 (+50%)	948,92 (+31,3%)	40,63 (+41,9%)	93,40 (-8,1%)	41,27 (+39,1%)

The variation in the compressive strength of concrete caused a significant effect on the axial load capacity (Figure 13a), the same has not observed on bending moment capacity (Figure 13b). There is a direct relationship between the compressive strength of concrete and the ultimate force on pure compression (Point A, Figure 13a): if the first is increased, the last also increase. However, the same effect showed not to be effective for increasing the ultimate moment capacity (Point B, Figure 13b). When the concrete strength exceeds 50 MPa, the difference between the ultimate values (normal force and moment) is reduced, also decreasing the influence of the compressive strength of concrete on the M- N pair of strength for high-strength concretes.

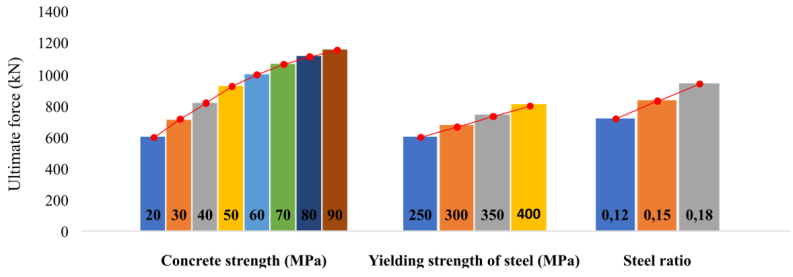

a) Effects on Ultimate Force – Point A (concentric load)

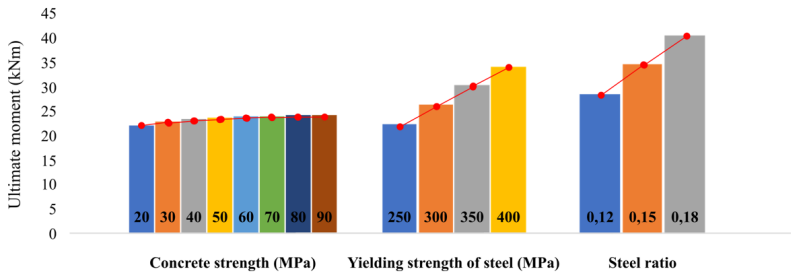

b) Effects on Ultimate Moment - Point B (pure bending)

Figure 13. Effect of variables on ultimate values of force and moment.

If the compressive strength of concrete or steel ratio have increases of 50% result on increases of 18,2% and 31,3% on the ultimate force for concentric load. Regarding to the values of ultimate moment (pure bending case), increases of 2,9% and 41,9% were observed respectively for strength of concrete and steel ratio. Similar effects were observed when the yielding strength of steel was increased in 40% (250 to 350 MPa): increase of 22,6% and 36,2% in the ultimate values of force and moment, respectively. Therefore, the results of parametric study allow to observe that the variables related to the steel profile (yield strength and steel ratio) had greater influence on the values of ultimate strength than the variation in the concrete strength.

Figure 14 shows the M-N interaction curves to consider the highest values of concrete strength and yielding strength of steel (90 MPa and 450 MPa, respectively) and thickness of the tube equal to 3 mm.

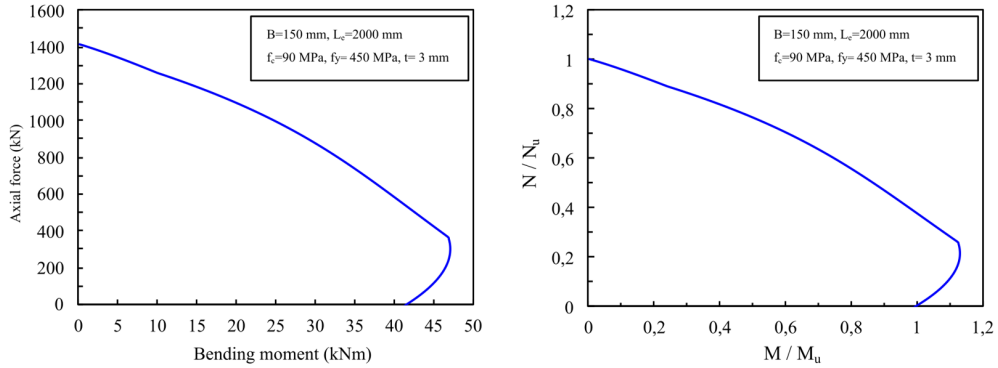

a) M-N interaction curve b) Dimensionless curve

Figure 14. Behavior of the M-N interaction curves for the highest values of concrete strength and yielding strength of steel.

Table 11 shows the M-N pairs of strength for Points A, B and D of the obtained M-N interaction curve.

Table 11. M-N pairs of strength for the highest values of concrete strength and yielding strength of steel.

Point A	Point B	Point D	
N (kN)	**M (kNm)**	**N (kN)**	**M (kNm)**
1417,4	41,5	300,8	47,07

The use of the highest strength values for steel and concrete resulted in the highest value of ultimate force on pure compression of the parametric study (Point A, Figure 14a and Table 11). Additionally, it was observed that the value of moment resistance at vertex D was 13,4% higher than the value of moment resistance at Point B (Figure 14b and Table 11). For all the analysis carried out, vertex D was more distant from Point B when there was an association of the lowest yielding strength of steel (250 MPa) and concrete C90 (Figure 11b).

5 CONCLUSIONS

This study presented a method for obtaining M-N interaction curves for rectangular concrete-filled steel tube columns. For this, was considered the strain compatibility method and a computational code was developed for rectangular concrete-filled subjected to uniaxial bending moments. The results of proposed method were coherent if compared to results of the literature [17], [18]. In comparison with literature results, the proposed model underestimated the M-N pairs of strength. On the other hand, in the comparison with Brazilian Standard Code [20] was observed an excellent correlation for compressive normal force (N_{Rd}) and moment strength M_{Rd} for both interaction models (I and II) when considering the beam-column strength. Additionally, in comparison with the simplified model of ABNT NBR 16239 [21], a good correlation was observed for moment strength M_{Rd}. The worst results were observed in the comparison of the proposed model with values of EN 1994-1-1 [22], especially for values of N_{Rd}. The proposed model presented regions in the M-N interaction curves that sometimes underestimated, sometimes overestimated the simplified curves of the standard code [20]–[22].

The influence of the compressive strength of concrete, yielding strength of steel and steel ratio on the eccentric compression strength was evaluated in a parametric study. Among the variables evaluated, those related to steel (yielding strength of steel and the steel ratio) contributed more significantly to the increase in the ultimate values of force and moment.

REFERENCES

[1] T. Fujimoto, A. Mukai, I. Nishiyama, and K. Sakino, "Behavior of eccentrically loaded concrete-filled steel tubular columns," *J. Struct. Eng.*, vol. 130, no. 2, pp. 203–212, 2004.

[2] P. Neogi, H. Sen, and J. Chapman, "Concrete-filled tubular steel columns under eccentric loading," *Struct. Eng.*, vol. 47, no. 5, pp. 187–195, 1969.

[3] R. Bridge, "Concrete filled steel tubular columns," *Civ. Eng. Trans.*, vol. 18, no. 2, pp. 127–133, 1976.

[4] H. Shakir-Khalil and J. Zeghiche, "Experimental behaviour of concrete-filled rolled rectangular hollow-section columns," *Struct. Eng.*, vol. 67, no. 19, pp. 346–353, 1989.

[5] M. Mouli, "*Behaviour of concrete-filled composite columns*," M.S. thesis, Univ. Manchester, Manchester, 1988.

[6] Q. Shan, J. Cai, X. Li, and J. Tan, "Analysis of concrete-filled square steel tube short columns under eccentric loading," *Math. Probl. Eng.*, vol. 2019, pp. 1–12, 2019.

[7] F. Yuan, H. Huang, and M. Chen, "Effect of stiffeners on the eccentric compression behaviour of square concrete-filled steel tubular columns," *Thin-walled Struct.*, vol. 135, pp. 196–209, 2019.

[8] D. Liu, "Behaviour of eccentrically loaded high-strength rectangular concrete-filled steel tubular columns," *J. Construct. Steel Res.*, vol. 62, no. 8, pp. 839–846, 2006.

[9], M. Kadhim, "Numerical modelling of concrete-filled stainless steel slender columns loaded eccentrically," *World J. Eng.*, vol. 17, no. 5, pp. 697–707, 2020., http://dx.doi.org/10.1108/WJE-09-2019-0268.

[10] X. Qu, Z. Chen, and G. Sun, "Experimental study of rectangular CFST columns subjected to eccentric loading," *Thin-walled Struct.*, vol. 64, pp. 83–93, 2013.

[11] E. Bonaldo, "Composite columns with high strength concrete core," M.S. thesis, Fac. Civ. Eng., State Univ. Campinas, 2001. [in Portuguese].

[12] J. Cai, J. Pan, C. Lu, and X. Li, "Nonlinear analysis of circular concrete filled steel tube columns under eccentric loading," *Mag. Concr. Res.*, vol. 72, no. 6, pp. 292–303, 2020.

[13] B. Uy, Z. Tao, and L.-H. Han, "Behaviour of short and slender concrete-filled stainless steel tubular columns," *J. Construct. Steel Res.*, vol. 67, no. 3, pp. 360–378, 2011.

[14] W. Li, L.-H. Han, and T.-M. Chan, "Performance of concrete-filled steel tubes subjected to eccentric tension," *J. Struct. Eng.*, vol. 141, no. 12, pp. 04015049, 2015.

[15] D. Hernández-Figueirido, M. L. Romero, J. L. Bonet, and J. M. Montalvá, "Ultimate capacity of rectangular concrete-filled steel tubular columns under unequal load eccentricities," *J. Construct. Steel Res.*, vol. 68, no. 1, pp. 107–117, 2012.

[16] S. De Nardin, "Concrete filled steel columns: a study of combined bending and compression and beam-column connections," Ph.D. dissertation, Eng. Sch. São Carlos, Univ. São Paulo, São Carlos, 2003. [in Portuguese].

[17] R. A. Melo, "Numerical analysis of the square concrete filled steel tube composite columns and under eccentric loads," M.S. thesis, Civ. Eng. Dep., Fed. Univ. São Carlos, São Carlos, 2018. [in Portuguese].

[18] Y. Du, Z. Chen, Y.-B. Wang, and J. Y. Richard Liew, "Ultimate resistance behavior of rectangular concrete-filled tubular beam-columns made of high-strength steel," *J. Construct. Steel Res.*, vol. 133, pp. 418–433, 2017.

[19] G. Li, B. Chen, Z. Yang, and Y. Feng, "Experimental and numerical behaviour of eccentrically loaded high strength concrete filled high strength square steel tube stub columns," *Thin-walled Struct.*, vol. 127, pp. 483–499, 2018.

[20] Associação Brasileira de Normas Técnicas, *Design of Steel and Composite Structures for Buildings*, NBR 8800:2008, 2008. [in Portuguese].

[21] Associação Brasileira de Normas Técnicas, *Design of Steel and Composite Structures for Buildings Using Hollow Sections*, NBR 16239:2013, 2013. [in Portuguese].

[22] European Committee for Standardization, *Eurocode 4: Design of Concrete Structures – Part 1-1: General Rules and Rules for Buildings*, EN 1994-1-1, 2004.

[23] Y. Bong Kwon and I. Kyu Jeong, "Resistance of rectangular concrete-filled tubular (CFT) sections to the axial load and combined axial compression and bending," *Thin-walled Struct.*, vol. 79, pp. 178–186, 2014.

[24] W. T. Hsu, D. M. Lue, and C. Y. Chang, "An investigation into the strength of concrete-filled tubes," *Appl. Mech. Mater.*, vol. 284-287, pp. 1208–1214, 2013.

[25] H.-J. Lee, I.-R. Choi, and H.-G. Park, "Eccentric compression strength of rectangular concrete-filled tubular columns using high-strength steel thin plates," *J. Struct. Eng.*, vol. 143, no. 5, 04016228, 2017.

[26] C.-H. Lee, T. H.-K. Kang, S.-Y. Kim, and K. Kang, "Strain compatibility method for the design of short rectangular concrete-filled tube columns under eccentric axial loads," *Constr. Build. Mater.*, vol. 121, pp. 143–153, 2016.

[27] Z. Lai, A. H. Varma, and K. Zhang, "Noncompact and slender rectangular CFT members: experimental database, analysis, and design," *J. Construct. Steel Res.*, vol. 101, pp. 455–468, 2014.

[28] A. Behnam and M. D. Denavit, "Plastic stress distribution method for predicting interaction strength of steel-concrete composite cross sections," *J. Construct. Steel Res.*, vol. 170, 106092, 2020.

[29] Associação Brasileira de Normas Técnicas, *Design of Concrete Structures – Procedure*, NBR 6118:2014, 2008. [in Portuguese].

[30] American National Standards Institute, *Specification for Steel Structural Buildings*, ANSI/AISC 360:16, 2016.

[31] T. Perea, R. Leon, J. Hajjar, and M. Denavit, "Full-scale tests of slender concrete-filled tubes: interaction behavior," *J. Struct. Eng.*, vol. 140, no. 9, 04014054, 2014.

[32] H.-J. Hwang, *Prefabricated Steel-Reinforced Concrete Composite Column – New Trends in Structural Engineering.* London: IntechOpen, 2018.

[33] R. D. Ziemian, *Guide to Stability Design Criteria for Metal Structures*, 6th ed. Hoboken: John Wiley & Sons, 2010.

[34] M. Malite, "Composite steel-concrete structures: column design," *Met. Constr. Sao Paulo*, vol. 4, no. 16, pp. 4–8, 1994. [in Portuguese].

Author contributions: MF: conceptualization, writing, formal analysis, methodology; SDN and FMAF: conceptualization, supervision, writing, formal analysis, methodology.

Editors: Bernardo Horowitz, Guilherme Aris Parsekian.